

Synthesis, Physical Properties, and Field-Effect Mobility of Isomerically Pure *syn*-/*anti*-Anthradithiophene Derivatives

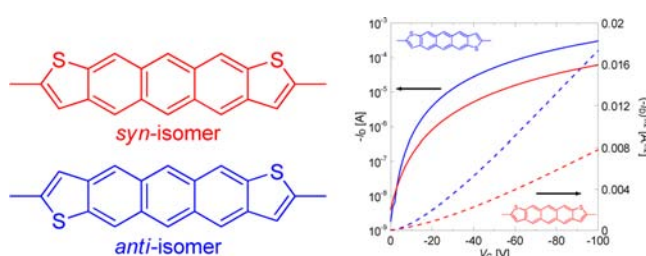
Masashi Mamada,* Tsukuru Minamiki, Hiroshi Katagiri, and Shizuo Tokito*

Graduate School of Science and Engineering, Yamagata University, Yonezawa,
Yamagata, 992-8510 Japan

mamada@yz.yamagata-u.ac.jp; tokito@yz.yamagata-u.ac.jp

Received June 13, 2012

ABSTRACT



Isomerically pure *syn*-/*anti*-isomers of 2,8-dimethylantrathiodithiophene (DMADT) were synthesized in five steps and characterized using thermogravimetry, X-ray single crystal analysis, UV–vis absorption, and electrochemical measurements. The physical properties in solution were slightly different for each isomer, whereby the more obvious differences were observed in the solid state. A field-effect transistor using the *anti*-isomer showed a much higher performance than that using the *syn*-isomer.

Fused heterocyclic aromatic hydrocarbons are known as semiconductors with high charge carrier mobilities and

(1) (a) Wang, C.; Dong, H.; Hu, W.; Liu, Y.; Zhu, D. *Chem. Rev.* **2012**, *112*, 2208. (b) Kuribara, K.; Wang, H.; Uchiyama, N.; Fukuda, K.; Yokota, T.; Zschieschang, U.; Jaye, C.; Fischer, D.; Klauk, H.; Yamamoto, T.; Takimiya, K.; Ikeda, M.; Kuwabara, H.; Sekitani, T.; Loo, Y.-L.; Someya, T. *Nat. Commun.* **2012**, *3*, 723. (c) Minemawaril, H.; Yamada, T.; Matsui, H.; Tsutsumi, J.; Haas, S.; Chiba, R.; Kumai, R.; Hasegawa, T. *Nature* **2011**, *475*, 364. (d) Uno, M.; Nakayama, K.; Soeda, J.; Hirose, Y.; Miwa, K.; Uemura, T.; Nakao, A.; Takimiya, K.; Takeya, J. *Adv. Mater.* **2011**, *23*, 3047. (e) Gelinck, G.; Heremans, P.; Nomoto, K.; Anthopoulos, T. D. *Adv. Mater.* **2010**, *22*, 3778.

(2) (a) Li, X.-C.; Sirringhaus, H.; Garnier, F.; Holmes, A. B.; Moratti, S. C.; Feeder, N.; Clegg, W.; Teat, S. J.; Friend, R. H. *J. Am. Chem. Soc.* **1998**, *120*, 2206. (b) Mamada, M.; Nishida, J.; Kumaki, D.; Tokito, S.; Yamashita, Y. *J. Mater. Chem.* **2008**, *18*, 3442. (c) Zhang, S.; Guo, Y.; Zhang, Y.; Liu, R.; Li, Q.; Zhan, X.; Liu, Y.; Hu, W. *Chem. Commun.* **2010**, *46*, 2841.

(3) (a) Gao, P.; Beckmann, D.; Tsao, H. N.; Feng, X.; Enkelmann, V.; Baumgarten, M.; Pisula, W.; Mullen, K. *Adv. Mater.* **2009**, *21*, 213. (b) Ebata, H.; Izawa, T.; Miyazaki, E.; Takimiya, K.; Ikeda, M.; Kuwabara, H.; Yui, T. *J. Am. Chem. Soc.* **2007**, *129*, 15732. (c) Izawa, T.; Miyazaki, E.; Takimiya, K. *Adv. Mater.* **2008**, *20*, 3388. (d) Takimiya, K.; Ebata, H.; Sakamoto, K.; Izawa, T.; Otsubo, T.; Kunugi, Y. *J. Am. Chem. Soc.* **2006**, *128*, 12604. (e) Gao, J.; Li, R.; Li, L.; Meng, Q.; Jiang, H.; Li, H.; Hu, W. *Adv. Mater.* **2007**, *19*, 3008. (f) Yamamoto, T.; Takimiya, K. *J. Am. Chem. Soc.* **2007**, *129*, 2224. (g) Mori, H.; Miyazaki, E.; Takimiya, K.; Ikeda, M.; Kuwabara, H. *Adv. Mater.* **2011**, *23*, 1222. (h) Appleton, A. L.; Miao, S.; Brombosz, S. M.; Berger, N. J.; Barlow, S.; Marder, S. R.; Lawrence, B. M.; Hardcastle, K. I.; Bunz, U. H. F. *Org. Lett.* **2009**, *11*, 5222.

have been a subject of considerable interest for organic electronics applications such as organic field-effect transistors (OFETs).¹ Most hydrocarbons in OFETs contain thiophene units due to their similarity in chemical structure to benzene rings and good stability against photo-oxidation.² In addition, the incorporation of heteroatoms enhances intermolecular interactions, resulting in excellent OFET device performance.³

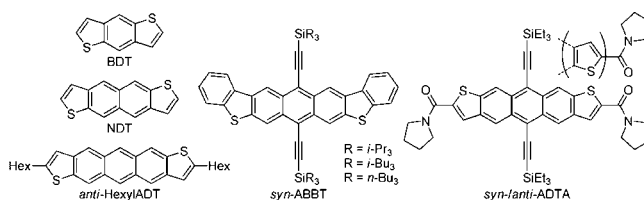
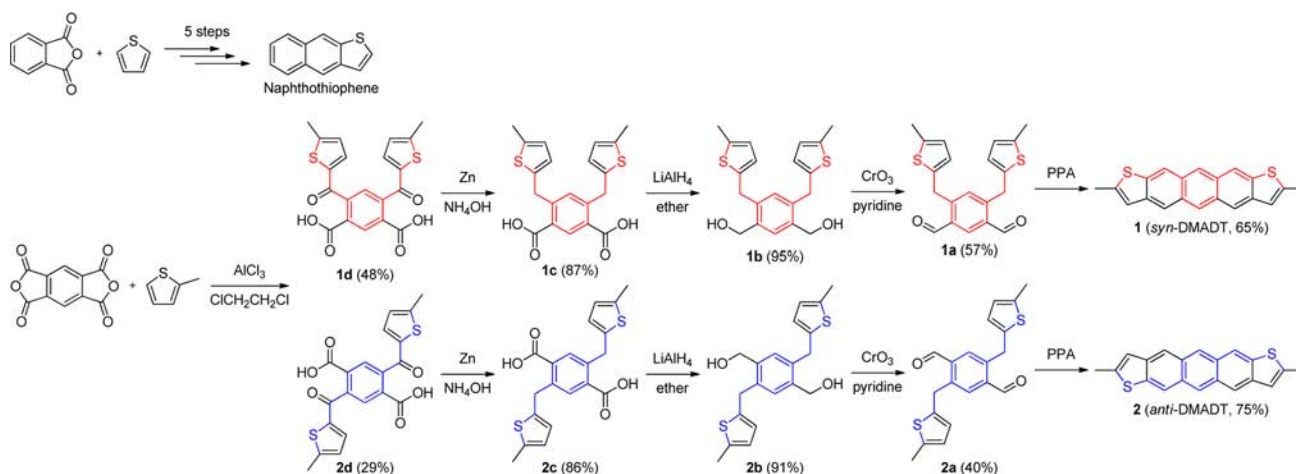


Figure 1. Structures of BDT, NDT, and ADT derivatives.

Benzodithiophene (BDT) and naphthodithiophene (NDT), which are heteroacenes corresponding to anthracene and tetracene, are useful as core structures of organic semiconductors or

Scheme 1. Synthesis of **1** (*syn*-DMADT) and **2** (*anti*-DMADT)



a building block for extended π -conjugation systems.^{4,5} Anthradithiophene (ADT) is analogous to pentacene, which is the most common organic semiconductor.⁶ ADT showed better stability than pentacene and good hole transporting properties.⁷ However, ADT is generally synthesized and used as a mixture of *syn*-/*anti*-isomers. Recently, several groups have obtained isomerically pure ADT derivatives, such as those shown in Figure 1. The pure *anti*-ADT derivatives which are substituted by alkyl groups were synthesized through a new synthetic route presented by Geerts et al.⁸ The synthetic method allows for a more detailed investigation of the characteristics of ADT derivatives, but it is limited to *anti*-derivatives. However, the pure *syn*-ADT derivatives (*syn*-ABBT) were developed and used as semiconductors by Tykwinski et al., although

extended π -conjugation systems were only synthesized.⁹ Anthony et al. synthesized both *syn*-/*anti*-ADT derivatives (ADTAs), and their performance in solar cells was investigated and compared for each isomer.¹⁰ However, those derivatives are substituted by large functional groups in order to separate them by recrystallization because ADT derivatives are basically insoluble. Thus, a synthetic approach to obtain simple and pure *syn*-/*anti*-ADTs and the comparison of their physical properties and FET characteristics for corresponding isomers are of significant interest. Herein, we report on a newly established synthesis method of pure *syn*-/*anti*-ADT derivatives and the comparison of their crystal structures and UV-vis absorption and redox potential measurements in solution as well as in the solid state. Also, FET device performance for each isomer is described.

The synthetic formulation strategy is based on the synthesis of a naphthothiophene ring, whereby the starting materials are phthalic anhydride and thiophene (Scheme 1).¹¹ The naphthothiophene ring can be considered a part of the ADT ring. Thus, pyromellitic dianhydride, which has two reaction sites, should provide the ADT ring as shown in Scheme 1. In this scheme, 2-methylthiophene was used because dimethyl-substituted ADT (DMADT) showed better semiconducting properties than ADT.^{7b} The first reaction step gave a mixture of a *meta*-isomer (**1d**) and *para*-isomer (**2d**), where the geometry of thiophene for ADT syntheses is fixed on the benzene ring. Therefore, key to this strategy is the separation of these compounds. Fortunately, similar isomers from pyromellitic dianhydride with benzene have been separated by

(4) (a) Laquindanum, J. G.; Katz, H. E.; Lovinger, A. J.; Dodabalapur, A. *Adv. Mater.* **1997**, *9*, 36. (b) Takimiya, K.; Kunugi, Y.; Konda, Y.; Niihara, N.; Otsubo, T. *J. Am. Chem. Soc.* **2004**, *126*, 5084. (c) Pan, H.; Li, Y.; Wu, Y.; Liu, P.; Ong, B. S.; Zhu, S.; Xu, G. *Chem. Mater.* **2006**, *18*, 3237. (d) Pan, H.; Wu, Y.; Li, Y.; Liu, P.; Ong, B. S.; Zhu, S.; Xu, G. *Adv. Funct. Mater.* **2007**, *17*, 3574. (e) Ebata, H.; Miyazaki, E.; Yamamoto, T.; Takimiya, K. *Org. Lett.* **2007**, *9*, 4499. (f) Wang, Y.; Parkin, S. R.; Watson, M. D. *Org. Lett.* **2008**, *10*, 4421. (g) Zhou, Y.; Lei, T.; Wang, L.; Pei, J.; Cao, Y.; Wang, J. *Adv. Mater.* **2010**, *22*, 1484.

(5) (a) Shinamura, S.; Osaka, I.; Miyazaki, E.; Nakao, A.; Yamagishi, M.; Takeya, J.; Takimiya, K. *J. Am. Chem. Soc.* **2011**, *133*, 5024. (b) Nakano, M.; Shinamura, S.; Houchin, Y.; Osaka, I.; Miyazaki, E.; Takimiya, K. *Chem. Commun.* **2012**, *48*, 5671. (c) Takimiya, K.; Shinamura, S.; Osaka, I.; Miyazaki, E. *Adv. Mater.* **2011**, *23*, 4347.

(6) Kelly, T. W.; Muires, D. V.; Baude, P. F.; Smith, T. P.; Jones, T. D. *Mater. Res. Soc. Symp. Proc.* **2003**, *2*, 678.

(7) (a) Laquindanum, J. G.; Katz, H. E.; Lovinger, A. J. *J. Am. Chem. Soc.* **1998**, *120*, 664. (b) Chen, M. C.; Kim, C.; Chen, S. Y.; Chiang, Y. J.; Chung, M. C.; Facchetti, A.; Marks, T. J. *J. Mater. Chem.* **2008**, *18*, 1029. (c) Jurchescu, O. D.; Hamadani, B. H.; Xiong, H. D.; Park, S. K.; Subramanian, S.; Zimmerman, N. M.; Anthony, J. E.; Jackson, T. N.; Gundlach, D. J. *Appl. Phys. Lett.* **2008**, *92*, 132103. (d) Jurchescu, O. D.; Subramanian, S.; Kline, R. J.; Hudson, S. D.; Anthony, J. E.; Jackson, T. N.; Gundlach, D. J. *Chem. Mater.* **2008**, *20*, 6733. (e) Payne, M. M.; Parkin, S. R.; Anthony, J. E.; Kuo, C.-C.; Jackson, T. N. *J. Am. Chem. Soc.* **2005**, *127*, 4986. (f) Subramanian, S.; Park, S. K.; Parkin, S. R.; Podzorov, V.; Jackson, T. N.; Anthony, J. E. *J. Am. Chem. Soc.* **2008**, *130*, 2706.

(8) Tylleman, B.; Velde, C. M. L. V.; Balandier, J.-Y.; Stas, S.; Sergeev, S.; Geerts, Y. H. *Org. Lett.* **2011**, *13*, 5208.

(9) Lehnerr, D.; Hallani, R.; McDonald, R.; Anthony, J. E.; Tykwinski, R. R. *Org. Lett.* **2012**, *14*, 62.

(10) Li, Z.; Lim, Y.-F.; Kim, J. B.; Parkin, S. R.; Loo, Y.-L.; Malliaras, G. G.; Anthony, J. E. *Chem. Commun.* **2011**, *47*, 7617.

(11) (a) Tedjamulia, M. L.; Tominaga, Y.; Castle, R. N. *J. Heterocycl. Chem.* **1983**, *20*, 1143. (b) Carruthers, W.; Douglas, A. G.; Hill, J. *J. Chem. Soc.* **1962**, 704.

recrystallization from acetic acid,¹² and the same method could be adopted for the separation of isomers **1d** and **2d**. The ratio of isomers **1d** and **2d** was 2:1, which is different from benzene derivatives. In the third step, the R_f values of isomers **1b** and **2b** on the silica gel plate were different when eluted with ethyl acetate due to a difference in polarity derived from their dipole moment. Thus, isomeric purity is high, even when a small amount of opposite isomers remain in the recrystallization for isomers **1d** and **2d**. The separated isomers **1d** and **2d** could be converted to DMADTs **1** and **2**, respectively, with good yields under the same reaction conditions used for the synthesis of naphthothiophene. Finally, the synthesis of DMADTs was successfully conducted through regiochemical control and the products were purified by sublimation. The solubility of these products in common organic solvents is relatively low.

TG-DTA for isomers **1** and **2** revealed decomposition above 400 °C, suggesting high thermal stabilities. The 5% weight losses were at temperatures of 424 and 440 °C for isomer **1** (*syn*-isomer) and isomer **2** (*anti*-isomer), respectively (see Supporting Information (SI)). The higher decomposition temperature for isomer **2** might be related to its different molecular structure as well as differences in intermolecular interactions.

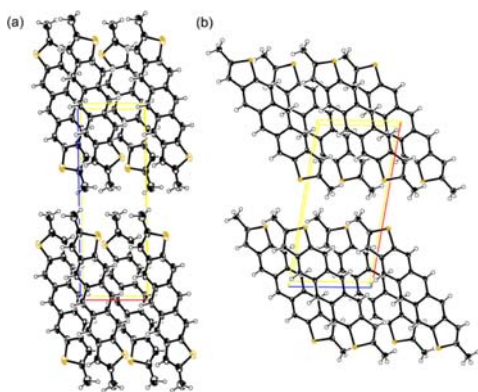


Figure 2. Crystal packing of (a) **1** and (b) **2** along with the *b*-axis (thermal ellipsoids 50% probability).

Single crystal structure analyses were carried out to confirm the molecular geometry and to investigate intermolecular interactions in the solid state (Figure 2). The crystals for isomers **1** and **2** were obtained by sublimation. Crystal growth was comparatively easier for isomer **2**. Compound **1** crystallizes in the noncentrosymmetric space group $P2_1$, whereby it forms twinned crystals and involves crystal disorder. On the other hand, the single crystal for isomer **2** contains centrosymmetric half-molecules (C_{2h}) in the asymmetric unit without disorder. A herringbone packing motif was observed for both isomers with a tilt angle of 52.1° for isomer **1** and 50.8° for isomer **2**. As shown in Figure 2, the molecular orientations are clearly

different. The molecules in isomer **2** are arranged with slipped herringbone packing, which slightly reduces the overlap between rings.

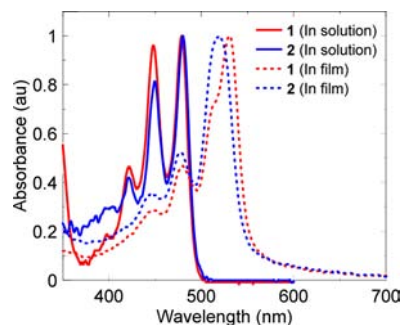


Figure 3. Normalized absorption spectra of isomers **1** and **2** in CH_2Cl_2 (solid line) and in film (dashed line).

Table 1. Optical and Electrochemical Properties

compd		λ_{abs} (nm) ^a	E_{ox1} (V) ^b	E_{ox2} (V) ^b	E_{red} (V) ^b	HOMO (eV) ^c	LUMO (eV) ^c
1	solution	479	0.23	0.78	-2.35	-5.03	-2.45
	calcd ^d	488	–	–	–	-4.70	-1.85
	film	530	0.38	0.83	-1.78	-5.18	-3.02
2	solution	480	0.23	0.77	-2.34	-5.03	-2.46
	calcd ^d	490	–	–	–	-4.69	-1.86
	film	519	0.36	0.80	-1.70	-5.16	-3.10

^aThe lowest energy maxima. ^bDetermined by differential pulse voltammetric measurement in 0.1 M solution of Bu_4NPF_6 in *o*-dichlorobenzene at 100 °C or in film with 0.1 M solution of Bu_4NPF_6 in CH_2Cl_2 at rt (vs Fc/Fc^+). ^cEstimated vs vacuum level from $E_{\text{HOMO}} = -4.80 - E_{\text{ox}}$ or $E_{\text{LUMO}} = -4.80 - E_{\text{red}}$. ^dCalculated by DFT methods at the B3LYP/6-31G(d,p) level using the Gaussian 09 program.

The optical and electrochemical properties for isomers **1** and **2** were investigated. The results are summarized in Figure 3 and in Table 1. The UV–vis spectra in solution showed a typical transition of ADT derivatives. The red shift of ca. 1 nm (65 cm^{-1}) was observed in isomer **2** (*anti*-isomer), and the spectra for each isomer were similar. The solubility is better for isomer **1** (*syn*-isomer). Thus, if a mixture was used for these measurements, the result would likely include more contributions from the *syn*-isomer. In fact, the reported absorption maximum of a mixture was 479 nm which corresponds to that for the *syn*-isomer.^{7b} The optical energy gaps estimated from the onset of the absorption are ca. 2.51 eV. The photooxidative stability level as determined by a decay in the absorbance was similar to the previously reported values (see SI).^{7b}

The absorption spectra in a 50-nm-thick film on a quartz plate showed clear differences in each isomer. Both isomers showed a large bathochromic shift in the absorption bands compared to the solution state, indicating the optical energy gaps of 2.25 eV for isomer **1** and 2.27 eV for isomer **2**.

(12) Du, D.; Jiang, Z.; Liu, C.; Sakho, A. M.; Zhu, D.; Xu, L. *J. Organomet. Chem.* **2011**, 696, 2549.

Interestingly, the lowest absorption maximum for isomer **1** (*syn*-isomer) appeared at an 11 nm longer wavelength compared to that for isomer **2** (*anti*-isomer). This is attributed to differences of intermolecular interactions.

The transition dipoles of molecules, calculated by the time-dependent density functional theory (TD-DFT) method, were in the direction of the molecular short axis for isomer **1**, as seen in acenes, and oblique to that for isomer **2**.^{13,14} Since the herringbone crystal packing is exhibited for both, the aggregation cannot be classified as *J*-type or *H*-type. In practice, the molecular orientations in single crystals and in thin films are not always identical. However, the XRD pattern of a thin film of isomer **1** suggested a *d*-spacing which is nearly equivalent to the length of the *c*-axis for a single crystal, whereas the thin film of isomer **2** exhibited almost the same *d*-spacing as isomer **1**, which alters the estimation from the single crystal. Therefore, at least isomer **1**, and most likely isomer **2**, can be considered to have a herringbone packing arrangement in a thin-film form. In this case, the nearest two molecules may lead to the band splitting into higher energy and lower energy contributions (Davydov splitting).¹⁵ Here, the lowest energy absorption peak at 520 nm of isomer **1** (*syn*-isomer) exhibited a Davydov component such as tetracene and pentacene,¹⁶ but isomer **2** (*anti*-isomer) showed a broad peak in the 0–0 band.

Differential pulse voltammetry (DPV) in solution for isomers **1** and **2** showed two oxidation peaks and a reduction peak (see SI). The first oxidation potential was 0.23 V vs Fc/Fc⁺ for both isomers, and the reduction potentials of isomers **1** and **2** were –2.35 and –2.34 V, respectively. The estimated HOMO–LUMO values from these redox potentials are summarized in Table 1. The HOMO–LUMO energy gaps are consistent with the optical energy gaps derived from UV–vis measurements. Although the redox potentials in solution were nearly the same for both isomers, those small differences revealed intermolecular interactions in film, as well as in the UV–vis spectra. The DPV measurements in thin films of isomers **1** and **2** showed two oxidation peaks and one weak reduction peak, which are similar in solution. These redox processes appeared as a positive shift of the results in solution. Since the shifts in the reduction peaks were larger, the LUMO levels are located at much deeper levels in the solid state. The HOMO levels for isomers **1** and **2** estimated from their oxidation potentials were similar.

The FET devices for both isomers were fabricated on a hexamethyldisilazane (HMDS)-treated substrate at rt with a top-contact device configuration (Figure 4). The devices for isomers **1** and **2** showed hole mobilities of 0.084 and

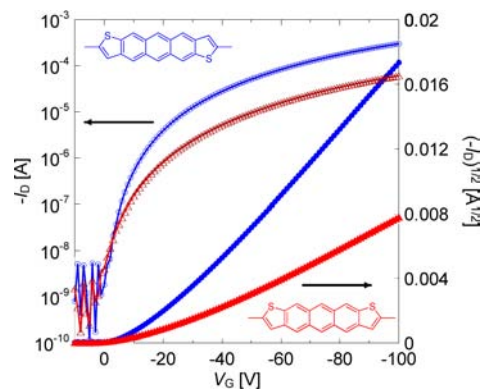


Figure 4. Transfer characteristics of *anti*-DMADT (blue lines, circles) and *syn*-DMADT (red lines, triangles).

0.41 cm² V^{−1} s^{−1}, respectively, which are higher than the previously reported mobility in a mixture (0.062 cm² V^{−1} s^{−1}).^{7b} Interestingly, the *anti*-isomer **2** exhibited a mobility that was five times higher than that for *syn*-isomer **1**, which is attributed to differences in their molecular structures, as well as to intermolecular interactions in their thin films. The mobility results for *syn*-/*anti*-isomers show the same tendencies as those for naphthodithiophenes, whereby the centrosymmetric derivatives showed higher mobilities than the axisymmetric ones.^{5a} These results clearly suggest the importance of separating isomers in FET devices.

In summary, pure isomers of anthradithiophene derivatives were successfully synthesized in good yields. The molecular structures for these isomers have been verified with X-ray single crystal structure analysis. We observed only slight differences in photochemical and electrochemical properties for each isomer in solution. However, apparent differences were observed in the solid state, especially in FET devices, whereby the *anti*-isomer showed higher device performance than the *syn*-isomer. Further investigation to understand these differences in the device performance is currently underway. This synthetic work enabled the detailed investigation of physical properties of ADT derivatives. The synthesis is applicable for pure isomers of unsubstituted-ADTs, dialkyl-ADTs, and dibromo-ADTs as building blocks for semiconductors.

Acknowledgment. This work was supported by the Japan Regional Innovation Strategy Program by the Excellence (creating international research hub for advanced organic electronics) of Japan Science and Technology Agency (JST), and by the Ministry of Education, Culture, Sports, Science and Technology, Japan.

Supporting Information Available. Full experimental details, characterization data, and CIF files for isomers **1** and **2**. This material is available free of charge via the Internet at <http://pubs.acs.org>.

The authors declare no competing financial interest.

(13) DFT calculations were carried out with Gaussian 09 program package: Frisch, M. J. et al. *Gaussian 09*, revision C.01; Gaussian, Inc.: Wallingford, CT, 2010; see SI for full reference.

(14) Lim, S.-H.; Bjorklund, T. G.; Spano, F. C.; Bardeen, C. J. *Phys. Rev. Lett.* **2004**, *92*, 107402.

(15) (a) Davydov, A. S. *Theory of molecular excitons*; Plenum Press, New York, 1971. (b) Kasha, M.; Rawls, H. R.; El-Bayoumi, M. A. *Pure Appl. Chem.* **1965**, *11*, 371.

(16) (a) Philpott, M. R. *J. Chem. Phys.* **1969**, *50*, 5117. (b) Maliakal, A.; Raghavachari, K.; Katz, H.; Chandross, E.; Siegrist, T. *Chem. Mater.* **2004**, *16*, 4980. (c) Miao, Q.; Nguyen, T.-Q.; Someya, T.; Blanchet, G. B.; Nuckolls, C. *J. Am. Chem. Soc.* **2003**, *125*, 10284.